ACCOUNTS of chemical research

Article

pubs.acs.org/accounts

Amorphous Metal–Organic Frameworks

Thomas D. Bennett* and Anthony K. Cheetham*

Department of Materials Science and Metallurgy, University of Cambridge, 27 Charles Babbage Road, Cambridge CB3 0FS, United Kingdom

CONSPECTUS: Crystalline metal–organic frameworks (MOFs) are porous frameworks comprising an infinite array of metal nodes connected by organic linkers. The number of novel MOF structures reported per year is now in excess of 6000, despite significant increases in the complexity of both component units and molecular networks. Their regularly repeating structures give rise to chemically variable porous architectures, which have been studied extensively due to their sorption and separation potential. More recently, catalytic applications have been proposed that make use of their chemical tunability, while reports of negative linear compressibility and negative thermal expansion have further expanded interest in the field.

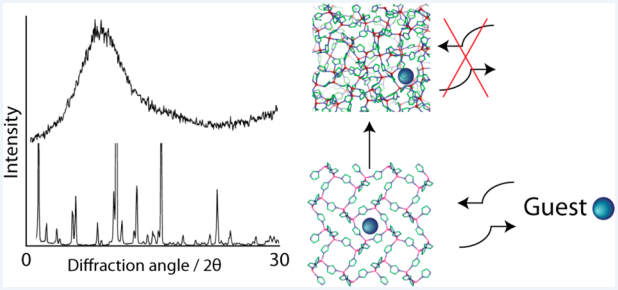

Amorphous metal–organic frameworks (*a*MOFs) retain the basic building blocks and connectivity of their crystalline counterparts, though they lack any long-range periodic order. Aperiodic arrangements of atoms result in their X-ray diffraction patterns being dominated by broad "humps" caused by diffuse scattering and thus they are largely indistinguishable from one another. Amorphous MOFs offer many exciting opportunities for practical application, either as novel functional materials themselves or facilitating other processes, though the domain is largely unexplored (total *a*MOF reported structures amounting to under 30).

Specifically, the use of crystalline MOFs to detect harmful guest species before subsequent stress-induced collapse and guest immobilization is of considerable interest, while functional luminescent and optically active glass-like materials may also be prepared in this manner. The ion transporting capacity of crystalline MOFs might be improved during partial structural collapse, while there are possibilities of preparing superstrong glasses and hybrid liquids during thermal amorphization. The tuning of release times of MOF drug delivery vehicles by partial structural collapse may be possible, and *a*MOFs are often more mechanically robust than crystalline materials, which is of importance for industrial applications.

In this Account, we describe the preparation of *a*MOFs by introduction of disorder into their parent crystalline frameworks through heating, pressure (both hydrostatic and nonhydrostatic), and ball-milling. The main method of characterizing these amorphous materials (analysis of the pair distribution function) is summarized, alongside complementary techniques such as Raman spectroscopy. Detailed investigations into their properties (both chemical and mechanical) are compiled and compared with those of crystalline MOFs, while the impact of the field on the processing techniques used for crystalline MOF powders is also assessed. Crucially, the benefits amorphization may bring to existing proposed MOF applications are detailed, alongside the possibilities and research directions afforded by the combination of the unique properties of the amorphous domain with the versatility of MOF chemistry.

■ INTRODUCTION

Crystalline metal–organic frameworks (MOFs) are network solids in which inorganic nodes (clusters or metal ions) are linked via organic ligands in an infinite array. The placement of these moieties within the framework is highly regular and as such the materials are said to possess long-range order.

The synthesis of novel MOF materials has been the subject of intense research and debate over the past decade, mainly because of their potential for application in gas storage and separation, catalysis, and sensing.[1] While the complexity and gas storage ability of novel MOFs is ever increasing, they are necessarily becoming more difficult to synthesize and characterize. This has led to a surge in work on functionalizing, altering, and utilizing existing MOF structures.

A small but growing number of noncrystalline MOFs are steadily capturing scientific interest (Table 1), though it is only recently that well-characterized examples of amorphous MOFs (*a*MOFs) have started to appear.[2] To date, they still remain woefully under represented, despite amorphization being well-known in inorganic materials and observed recently in porous aromatic frameworks.[3]

Amorphous MOFs may find applications in multiple areas, especially those that might involve the collapse of porous MOF structures around guest species. Reversible gas storage using pressure-induced amorphization[4] and irreversible long-term harmful substance storage[5] have already been suggested, while

Received: January 26, 2014
Published: April 7, 2014

   dx.doi.org/10.1021/ar5000314 | *Acc. Chem. Res.* 2014, 47, 1555–1562

release times of drug-loaded MOFs[6] might also be tailored using partial amorphization. In addition, zeolite collapse has been shown to produce inorganic glasses,[7] and similar processes might be used as routes to functional hybrid glasses. A third route of exploration involves understanding the process of amorphization itself (thermal or pressure-induced), in order to provide greater insight into the processing of MOF powders (sintering and densification).

The majority of work to date has been performed on a subfamily of MOFs called zeolitic imidazolate frameworks (ZIFs), which consist of tetrahedral metal centers (typically Zn^{2+} or Co^{2+}), connected by imidazolate ($C_3H_3N_2^-$) organic ligands.[8] The similarity of the angle subtended at these ligands to its counterpart Si−O−Si angle in inorganic zeolites results in ZIFs adopting similar network structures (Figure 1).

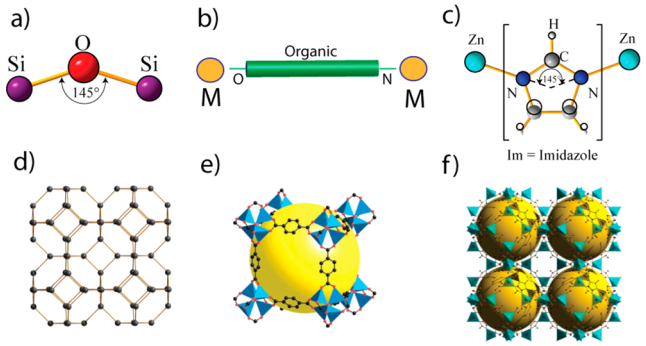

Figure 1. (a) The basic Si−O−Si building unit in inorganic zeolites, (b) M−L−M connectivity in MOFs, where the metal-coordinating atoms are usually N or O, (c) the M−Im−M building unit of zeolites, (d) the sodalite network topology of zeolites and ZIFs (gray atoms representing the metal nodes and yellow sticks representing the O or Im units linking them together), (e) unit cell of the prototypical MOF-5 (Zn_4O polyhedra, blue; C, black; yellow sphere representing the accessible area within the porous system), and (f) unit cell of ZIF-8 (ZnN_4 polyhedra, blue).

For simplicity, we define an amorphous MOF as a network of inorganic nodes (clusters or metal ions), linked by organic ligands (generally containing carboxylate or nitrogen-based functional groups). Crucially (and clearly differentiating them from crystalline MOFs), there is no long-range order within the structure, resulting in an absence of Bragg peaks in their X-ray or neutron diffraction patterns (Figure 2).

To date, approximately 30 cases of *a*MOFs have been reported, along with a minority of partially crystalline MOFs. Most have been prepared by ourselves through application of stress to a crystalline framework, though direct formation from inorganic salt and organic precursor (e.g., MOF aerogels[9]) has been observed in a minority of cases, as has their *in situ* formation during crystalline MOF synthesis.[10]

A summary of existing *a*MOFs is given in Table 1, sections a and b, where the prefixes a_p, a_m, a_T, and a_e are used to denote amorphization by pressure, ball milling, heating, or electrical discharge, respectively. In this Account, we describe various methods of preparing amorphous MOFs and the methods used to characterization them, their properties, and potential applications.

IDENTIFICATION AND CHARACTERIZATION

The absence of conventional Bragg diffraction from amorphous MOFs precludes determination of the position of individual

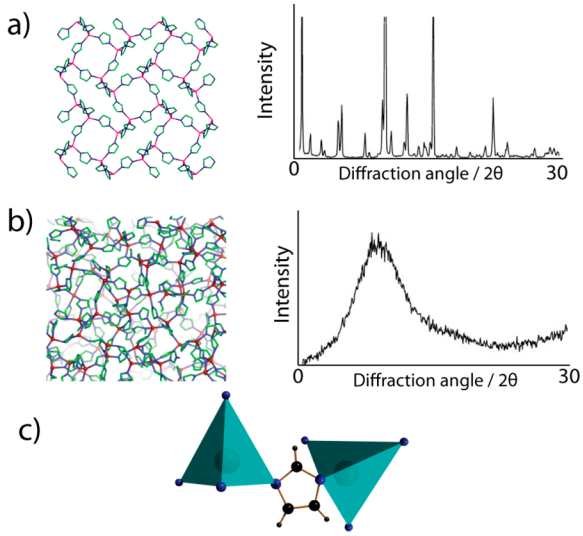

Figure 2. (a) Unit cell and associated X-ray diffraction pattern of ZIF-1 [$Zn(Im)_2$] and (b) comparably sized configuration of an amorphous ZIF and powder pattern. Zn, pink; C, green; N, blue; H atoms omitted. (C) The ZnN_4 tetrahedra (blue) and bridging imidazolate linker common to both crystalline and amorphous species.

atoms and thus the long-range structure of a material. The disordered nature of *a*MOFs does, however, give rise to diffuse scattering, which contains valuable information on two-atom interactions and can be used to yield insight into short and medium range ordering. The pair distribution function (PDF), $G(r)$, is in effect a map of atom−atom distances and can be used to ascertain the degree of local and intermediate ordering within amorphous solids, provided that the density and composition of the system in question is known. Indeed, the limit of ordering within an amorphous solid is made quickly apparent by the absence of features over a certain length scale (Figure 3).

X-ray or neutron total scattering experiments are performed to yield the total scattering function ($S(Q)$), which includes information on both Bragg and diffuse scattering. After suitable data reduction, the Fourier transform of $S(Q)$ yields the PDF, which can then be used to provide first insight into structural behavior.

Reverse Monte Carlo (RMC) modeling on PDF data using the RMC profile program can be used to build structural models of amorphous systems, though the modeling requires a starting configuration that is subsequently refined (in a manner largely analogous to Rietveld refinement) against the experimental data. The technique is more commonly used to probe disorder in crystalline systems,[25] though it has also been used to provide information on the *in situ* changes of a system under nonambient conditions.[26,27] Nevertheless, for amorphous solids that meet the criteria of known density and composition (most commonly due to it being formed from a known crystalline starting framework), PDF analysis remains the quintessential tool in the characterization of amorphous solids.

Aside from total scattering experiments, infrared and Raman spectroscopy may be used to identify the presence of various moieties and infer short-range ordering,[19,21] while differential scanning calorimetry (DSC) has been shown to indicate heating-induced amorphization in several publications.[12]

dx.doi.org/10.1021/ar5000314 | *Acc. Chem. Res.* 2014, 47, 1555−1562

Table 1. Reported *a*MOFs[a]

name	composition	amorphization conditions	space group of starting MOF	ref
		(a) Incorporating an Imidazolate-Type Ligand		
a_mZIF-1	$Zn(Im)_2$	25 Hz, 30 min	$P2_1/n$	11
a_TZIF-1		300 °C	$P2_1/n$	12
a_mZIF-3	$Zn(Im)_2$	25 Hz, 30 min	$P4_2/mnm$	11
a_TZIF-3		300 °C	$P4_2/mnm$	12
a_mZIF-4	$Zn(Im)_2$	25 Hz, 30 min	*Pbca*	11
a_TZIF-4		300 °C	*Pbca*	12
a_pZIF-4		0.35−0.98 GPa	*Pbca*	4
a_mCoZIF-4	$Co(Im)_2$	25 Hz, 30 min	*Pbca*	11
a_TCoZIF-4		300 °C	*Pbca*	12
a_mZIF-8	$Zn(mIm)_2$	25 Hz, 30 min	*I*43*m*	13
a_pZIF-8		0.34 GPa	*I*43*m*	14
a_mZIF-69	Zn(nIm)(cbIm)	25 Hz, 30 min	$P6_3/mmc$	5
a_mZIF-mnIm	$Zn(mnIm)_2$	25 Hz, 30 min	*I*43*m*	5
*a*Zn(ICA)-2[b]	$Zn(ICA)_2$	direct preparation	*d*	15
a_TNickel(II) bisimidazolate	$Ni(Im)_2$	decomposition 150 °C [Ni(acac)$(Im)_2$]	$P2_1/a$	16
a_TPalladium(II) bisimidazolate	$Pd(Im)_2$	decomposition 150 °C $Pd(Him)_2(Im)_2$	*Pnca*	16
a_TPlatinum(II) bisimidazolate	$Pt(Im)_2$	Decomposition 250 °C $Pt(Him)_2(Im)_2$	$P2_1/c$	16
a_TCopper(II) bisimidazolate	$Cu(Im)_2$	decomposition 110 °C $Cu(Him)_2(CO_3)_2{\cdot}H_2O$	*P*1	17
a_TRho-ZMOF	$Na_{48}In_{48}(HIMDc)_{96}$	200 °C	*Im*3*m*	18
		(b) Not Containing an Imidazolate Ligand		
a_pMOF-5	$Zn_4O(BDC)_3$	10.3 MPa, not hydrostatic	*Fm*3*m*	19
a_eMOF-5[c]	$Zn_4O(BDC)_3$	electrical discharge	*Fm*3*m*	20
*a*MOF-177[c]	$Zn_4O(BTB)_2$	compression	*P*31*c*	21
*a*Zn$(CN)_2$	Zn(CN)2	3 GPa (and X-ray exposure)	*P*43*m*	22
$a_T[ZnI_2]_3(TPT)_2]$	$[ZnI_2]_3(TPT)_2]$	200 °C	*C*2/*c*	23
$a_T[ZnBr_2]_3(TPT)_2]$	$[ZnBr_2]_3(TPT)_2]$	200 °C	*C*2/*c*	24
$a_T[ZnCl_2]_3(TPT)_2]$	$[ZnCl_2]_3(TPT)_2]$	200 °C	*C*2/*c*	24
$Fe_3O(BTC)_2F{\cdot}H_2O$ aerogel[b]	$Fe_3O(BTC)_2F{\cdot}H_2O$	direct preparation	*d*	9

[a]Im, imidazolate ($C_3H_3N_2^-$); mIm, 2-methylimidazolate ($C_4H_5N_3^-$); nIm, 2-nitroimidazolate ($C_3H_2N_3O_2^-$); cbIm, 5-chlorobenzimidazolate ($C_7H_4N_2Cl^-$); mnIm, 4-methyl-5-nitroimidazolate ($C_4H_4N_3O_2^-$); ICA, imidazolate-2-carboxaldehyde ($C_4H_3N_2O^-$); ImDC, imidazole-4,5-dicarboxylate ($C_5HN_2O_4^-$); BDC, benzene-1,4-dicarboxylate ($C_8H_3O_4^{2-}$); BTB, 1,3,5-tris(4′-carboxyphenyl)benzene ($C_{21}H_{15}O_6^{3-}$); TPT, 2,4,6-tris(4-pyridyl)triazine) ($C_{18}H_{12}N_6$). [b]Indicates *a*MOF reported synthesized directly from its precursors. [c]Indicates those cases where the X-ray diffraction pattern still contains some Bragg reflections. [d]Not applicable.

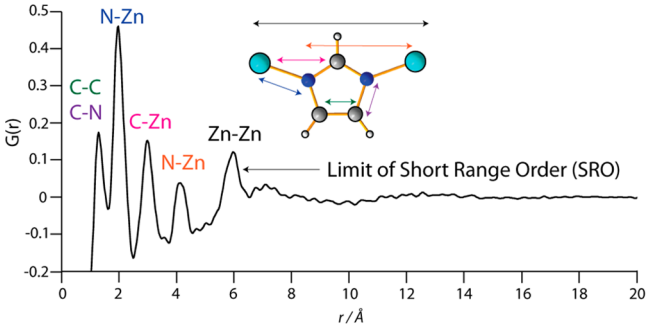

Figure 3. *G*(r), the Fourier transform of the *S*(Q) produced from an X-ray total scattering experiment on a_TZIF-4 [Zn$(Im)_2$]. The peaks correspond to distances between atom pairs, with the limit of correlated distances coming at 6 Å. The absence of defined features beyond this distance indicates the lack of any longer range ordering.

SYNTHESIS

Currently, identification of amorphous products when screening for novel MOF structures is not pursued, and it is highly likely that many have been synthesized and subsequently discarded without investigation. Indeed, with the application of high throughput screening, software has been developed with the aim of disregarding information on *a*MOFs with alarming readiness.[28] Despite this, limited information does exist on the direct synthesis of *a*MOFs, with fast rates of addition of triethylamine to zinc nitrate and ICA in *N*,*N*-dimethylformamide (DMF) yielding a disordered material and not the crystalline product formed with slow addition.[15]

More commonly, *a*MOFs are formed from the application of stress to crystalline frameworks. Some M^{II} imidazolate-containing complexes partially decompose upon heating to give the $M(Im)_2$ product.[16,17] The loss of inherent parts of the structure is not however a prerequisite for amorphization, as illustrated in a family of zinc tris(4-pyridyl)triazine-containing frameworks, which first lose solvent and then undergo amorphization at 473 K in separate demarcated steps, before a reconstructive transition at 573 K into a different framework.[24] This bears remarkable resemblance to the sequence of transitions discovered in ZIFs.[12]

Pressure has also been used to amorphize crystalline MOFs, with the prototypical framework MOF-5 (IRMOF-1) collapsing under just 3.5 MPa compression in a hydraulic press,[19] Raman spectroscopy being used to note the presence of similar vibrational modes across crystalline and amorphous products (thereby confirming the retention of local structural modes).[29] MOF-177, which shows large gas uptake capacities, undergoes similar collapse upon mechanical compression.[21] In both cases, collapse was observed to result in a large decrease in framework porosity. Amorphization of MOF-5 by electrical discharge

dx.doi.org/10.1021/ar5000314 | *Acc. Chem. Res.* 2014, 47, 1555−1562

similarly results in densification, with collapse linked to the destruction of metal-binding carboxylate groups in the framework. The presence of Bragg peaks at the point of amorphization however suggests, at best, an incomplete process.[20]

The role of radiation in amorphization processes has not yet been probed extensively, though interestingly the simple cyanide $Zn(CN)_2$ collapses at a pressure of 3 GPa, when exposed to X-rays but not without.[22] In general, the reaction of frameworks to a combination of stresses has not been researched. While the synthesis of MOFs by ball-milling is achieving greater scientific relevance, few reports exist where it is used to facilitate the collapse of frameworks.[11]

AMORPHOUS ZEOLITIC IMIDAZOLATE FRAMEWORKS

The vast majority of work done on amorphous MOFs has been undertaken on members of the ZIF subfamily. The prototypical example of temperature-induced amorphization in hybrid frameworks remains that of ZIF-4. This framework of composition $Zn(Im)_2$, which adopts the same network topology as the mineral $CaGa_2O_4$, contains *N*,*N*-dimethylformamide (DMF) molecules within its porous structure when synthesized solvothermally. Upon heating to ca. 200 °C, this pore-occupying solvent is lost, though the framework remains intact despite the fact that the pore apertures (at 2.1 Å diameter) are too small for the molecule to pass through. Upon further heating to ca. 300 °C, an irreversible transition to a dense topologically disordered phase with the same composition as crystalline ZIF-4 is observed. This phase was termed a_TZIF-4. Further heating to ca. 450 °C results in the crystallization of the most dense crystalline ZIF, ZIF-zni ($[Zn(Im)_2]$, zni referring to the network topology, which is identical to that adopted by zinc iodide), which is essentially nonpermeable.

Neutron total scattering data were collected *in situ* using the GEM diffractometer at the ISIS spallation source, and RMC Profile was used to model the crystalline−amorphous−crystalline transition. Starting structures based on ZIF-4 and ZIF-zni configurations were not able to produce a structural configuration that matched $G(r)$ for the amorphous ZIF, while a model derived from a random distribution of atoms similarly failed to converge on a chemically reasonable configuration. A model based on the continuous random network (CRN) model of silica glass (with distances altered to allow for the greater size of imidazolate compared with oxygen) afforded excellent fits to the observed data after refinement, though constraints on Zn coordination number and bond distances were used.[2]

Other zeolitic imidazolate frameworks (ZIF-1 and ZIF-3) of the same $Zn(Im)_2$ composition, with the zeolitic topologies BCT and DFT, respectively, were observed to undergo similar irreversible, reconstructive transitions. Amorphization in each case occurred after solvent removal and further heating of the evacuated framework, before recrystallization to the same dense ZIF-zni phase. Total scattering experiments were performed using Ag X-ray radiation (λ = 0.561 Å), Fourier transform of the almost-identical $S(Q)$ yielding $G(r)$s with no significant differences (Figure 4). The retention of short-range ordering (SRO) is evidenced in each case by the major peak in the PDF at ca. 6 Å, which corresponds to the M−M nearest neighbor pair. While the debate of the exact origin of the first sharp diffraction peak in total scattering experiments continues, some

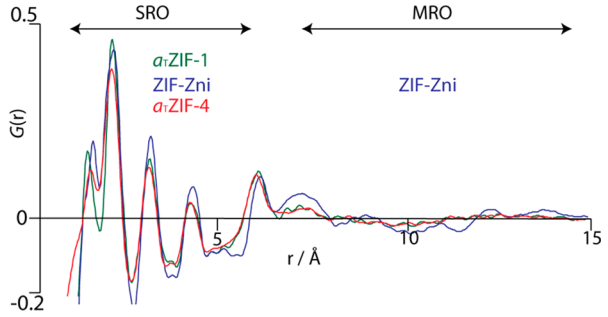

Figure 4. $G(r)$ for a_TZIF-1 (green), a_TZIF-4 (red), and ZIF-zni (blue).

have used it to define a "coherence length", which we approximate to be around 10 Å in ZIFs.[12]

Given our observations on a subset of $M(Im)_2$ frameworks, we would expect others to undergo similar processes, though no further experiments were performed. However, five ZIFs incorporating substituted imidazolate ligands were chosen and found to be thermally stable to ca. 500 °C. Efforts are continuing to separate the topological and steric factors that may influence amorphization in ZIFs.

The fate of those frameworks incorporating both simple and substituted imidazolate ligands upon heating has not yet been researched in detail, though their thermal stabilities are known to be generally below those of other ZIFs, which contain only one type of ligand.[8] Similarly, the role of the inorganic moiety in such amorphization processes remains unexplored. Frameworks in which alternating Li^+ and B^{3+} or Cd^{2+} cations replace Zn^{2+} do exist, though none are isostructural to ZIFs, which amorphize on heating.

Dehydrated crystalline ZIFs have also been observed to undergo amorphization by ball-milling. To enable accurate comparisons with the a_TZIFs, ZIF-1, -3, and -4 were subjected to ball-milling. Rapid, irreversible collapse was observed, though recrystallization into the dense ZIF-zni did not occur. Their PDFs were found to be extremely similar to those of the a_TZIFs, and indeed, all the evidence thus far points to the same amorphous products being formed from both routes. Further evidence comes from the fact that while recrystallization of the dense ZIF-zni during milling of an amorphous ZIF is not observed, the a_mZIFs can be heated to 450 °C to give the same crystalline products as the a_TZIFs.

Helium pycnometry was used to measure the densities of the crystalline and amorphous ZIFs, yielding values for the *a*ZIFs intermediate between those of ZIF-4 and ZIF-zni. No significant differences in density were observed between a_TZIFs and a_mZIFs of the same composition.

The intermediate nature of *a*ZIF-4 was further investigated in solution calorimetric experiments, which revealed relative enthalpies of formation of 8.61 and 4.1 kJ mol^{-1} for ZIF-4 and a_TZIF-4 (relative to ZIF-zni), indicating that the amorphization of ZIF-4 is exothermic in nature.[30]

Differences between the amorphization mechanisms must however exist, given the applicability of ball-milling induced amorphization to other ZIFs, including the prototypical ZIF-8 (Figure 5).[13] When subjected to the same treatment as its unsubstituted counterparts, the same rapid amorphization process was evident, despite the fact that it does not undergo structural collapse upon heating.

Unsurprisingly, upon study of a_mZIF-8 by PDF analysis, similarities in the SRO with a_mZIF-4 were evident, with the PDFs being featureless at greater distances aside from a broad

dx.doi.org/10.1021/ar5000314 | Acc. Chem. Res. 2014, 47, 1555−1562

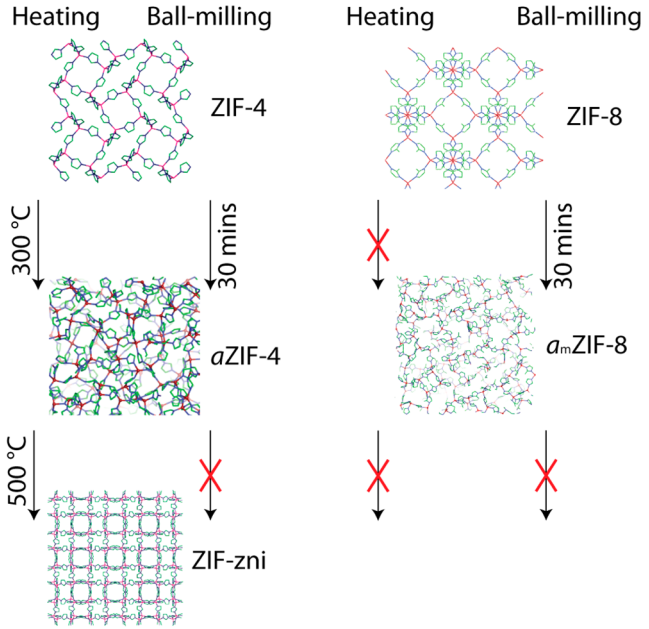

Figure 5. The different amorphization routes possible using unsubstituted ZIFs (e.g., ZIF-4) and those incorporating substituted linkers (e.g., ZIF-8).

low intensity hump at ca. 13 Å. This feature was observed to move slightly between the two, which was matched in the shift in position of the Zn−Zn distance at 6 Å. The structural configuration of a_mZIF-8 was elucidated using RMC modeling, with the same starting model as that used to produce the configuration of a_TZIF-4 (though slightly altered to account for the extra $-CH_3$ group) again enabling good fits to the experimentally observed total scattering structure factor for a_mZIF-8.

Multiple other ZIFs have been amorphized this way, including mixed ligand systems (ZIF-69) and those with large, bulky organic moieties such as benzimidazolate (ZIF-9). This susceptibility to collapse has been ascribed to their low shear modulus[31] and is presumably the reason why previous attempts to prepare catalytic mixtures with ZIFs have repeatedly failed.[32]

Zeolitic imidazolate frameworks display interesting behavior under hydrostatic pressure, with behavior largely dependent on the molecular size of the pressure-transmitting fluid. ZIF-8 undergoes irreversible amorphization at approximately 1.4 GPa in Fluorinert or 0.34 GPa under nonhydrostatic conditions. Use of ethanol as the hydrostatic medium was observed to delay amorphization (which still occurred at pressures significantly less than those required to amorphize its purely inorganic sodalite counterpart ($Na_8[Al_6Si_6O_{24}]Cl_2$)). PDF data collected on samples of crystalline and pressure-amorphized ZIF-8 suggest a retention of the Zn−imidazolate−Zn link (6 Å). Gas sorption measurements confirm a retention of porous structure, indicating a displacive transition. Infrared spectroscopy has been used to show that the effects of pressure upon ZIF-8 up to 1.6 GPa are entirely reversible, though pressures above this (and up to 39 GPa) resulted in recovery of a disordered product at ambient pressure.[33]

The behavior of ZIF-4 under pressure is similarly complex. The structure undergoes amorphization in both ethanol and a large molecule pressure-transmitting fluid, which is slowed by the presence of pore-occupying species.[4] The pressure of amorphization of an evacuated powder sample of ZIF-4 in the latter fluid is comparable to that of ZIF-8 at approximately 0.35 GPa. The absence of a transition to the dense ZIF-zni in the pressure range investigated suggests that the amorphization process proceeds with retention of the metal tetrahedra and associated structural connectivity. a_pZIF-4 is therefore unlikely to adopt the same CRN topology as those that have been thermally amorphized, which is a similar situation to classical amorphous zeolites.

The cause of pressure-induced instability in ZIFs is believed to be shear mode softening; molecular dynamics simulations show rapid decreases in some elastic constants upon compression in each case.[34]

PROPERTIES

BET analysis on substituted a_TZIFs and a_mZIFs indicates negligible porosities compared with crystalline frameworks (Figure 6a), in line with their increased densities relative to the crystalline phases.

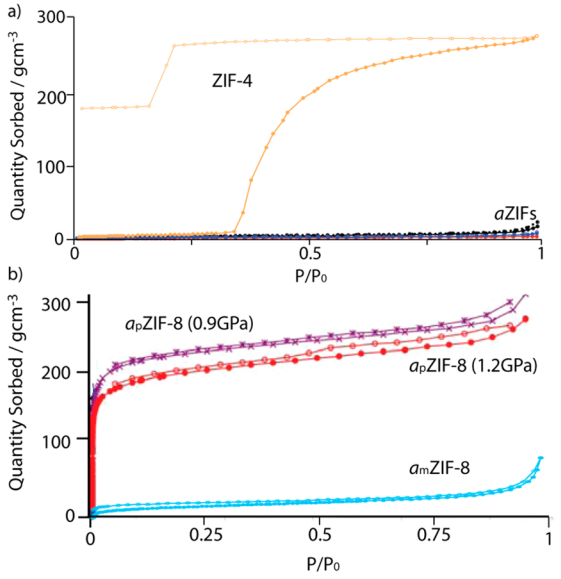

Figure 6. (a) N_2 sorption isotherms for a_mZIF-1 (black), a_mZIF-3 (red), a_mZIF-4 (green), and ZIF-4 (orange). (b) N_2 sorption isotherms for a_mZIF-8 (blue) and a_pZIF-8 amorphized at 0.9 GPa (purple) and 1.2 GPa (red). Closed circles indicate adsorption data, and open ones indicate desorption data.

Differences do however arise when we consider the gas sorption abilities of a_pZIF-8 and a_mZIF-8. Upon pressure-induced amorphization, the total gas uptake of ZIF-8 is reduced substantially (Figure 6b), though it is still comparable to that of crystalline ZIF-4. The evolution of ZIF-8 pore shape up to the point of amorphization reveals that the larger pores are essentially intact (though the channels linking them become more constricted),[35] while the nonporous nature of a_mZIF-8 may be caused by either structural densification or blocking of pore channels. This basic evidence suggests that at least at modest pressures, a_pZIF-8 and a_mZIF-8 possess different structures.

The mechanical properties of ZIFs are important,[36,37] given potential applications in electromechanical conversion and as thin films in chemical sensing and actuators. While the reduction in surface area upon milling prohibits study of a_mZIFs, the mechanical properties of a_TZIF-1 and a_TZIF-4

dx.doi.org/10.1021/ar5000314 | Acc. Chem. Res. 2014, 47, 1555−1562

(both Zn and Co analogues) were found to be the same (Figure 7a) and isotropic[2] (as one might expect given their

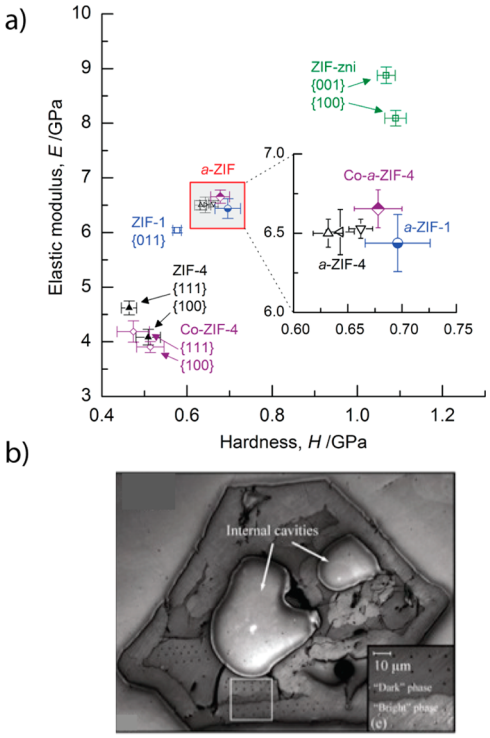

Figure 7. (a) Nanoindentation studies on ZIFs, data taken from prior literature and for indentation depths over 150 nm.[2,12] (b) Optical microscopy performed on a sample of ZIF-4 obtained by heating a single crystal to 300 °C.

isotropic CRN topology and the similarities in their PDFs). The stiffness was found to be approximately intermediate between the two bounding crystalline phases (i.e., increasing upon amorphization), which agrees with the greater densities of the amorphous frameworks,[37] though the hardness varies little. The dramatic change in Young's modulus may be beneficial in devices that detect subtle changes in conditions through amorphization (humidity, heat, or radiation sensors).

Some evidence of macroscopic flow during the crystalline ZIF-4 to a_TZIF-4 transition is presented by optical microscopy on a single crystal of a_TZIF-4 (Figure 7b). The crystal, heated to 300 °C at ambient pressure, clearly exhibits curved interior and exterior edges. The extent of isothermal flow on crystal morphology has not yet been researched, though the careful application of temperature and pressure to a large crystal of ZIF-4 may result in more drastic changes in morphology.

The isotropic mechanical response of the *a*ZIFs has implications for their thermal, electrical, and ion conductivity. While little work has been done on this area of MOFs, one would expect similarly isotropic responses of the materials upon amorphization. Through comparison with crystalline and amorphous SiO_2, we might also predict the *a*ZIFs to have higher, thickness-independent resistivities.

APPLICATIONS

The use of crystalline−amorphous transitions to facilitate different processes has enormous potential. One avenue currently being explored is the application of pressure-induced amorphization to reversibly store gas. In such applications, low, industrially accessible pressures of collapse are used to change the properties of the porous material. However, although reversible transitions have been found at low pressures, the a_pMOF formed is itself still porous and not a truly closed form (allowing for movement and possible diffusion of gas molecules into the environment).[14]

More promising is work on using crystalline ZIFs as hosts for "harmful" guest molecules and then collapsing the framework around the guest. The process renders the guest "trapped" within the porous interior, with channels (which formerly linked the pores to the outer surface) now blocked due to the introduction of substantial disorder. ZIF-8 was shown to display good molecular I_2 (a radioactive version of which is a nuclear fission byproduct) uptake capacity, retaining the guest upon *irreversible* pressure or ball-milling induced amorphization. Whereas the initial amounts of I_2 adsorbed in each case was comparable, there were slight differences in the ability of a_mZIF-8 and a_pZIF-8 to retain I_2 upon heating, with the former appearing to show better isothermal retention of I_2 at 200 °C.[5,38] Other ZIFs have also been found to display promising storage behavior, with a_mZIF-mnIm (mnIm referring to the imidazolate linker) in particular showing particularly striking retention of I_2 compared with the crystalline form (Figure 8).[5]

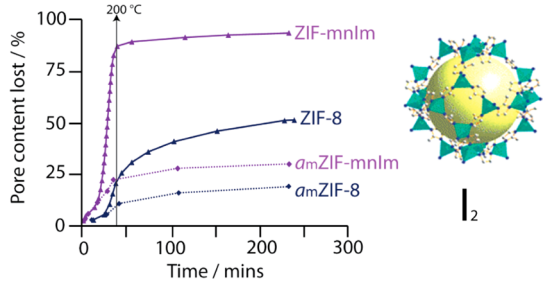

Figure 8. Isothermal thermogravimetric analysis (TGA) traces showing the retention of molecular I_2 by ZIF-8 and ZIF-mnIm.

As yet, solutions for reuse of the amorphized material have not yet been proposed, though, given the instability of ZIFs in acid[30] and work on the room temperature synthesis of ZIFs, one might anticipate dissolution of the amorphous product before the use of pH chemistry to reform the crystalline framework.

Biomedical applications of MOFs are of current interest, because some exhibit good drug storage capacities and hence potential for use as drug delivery vehicles.[6] Whereas the retention of guest is essential in the trapping applications mentioned above, here we look to the ability of a MOF to release its contents slowly and uniformly. It might be here that partial amorphization can play a role in tailoring release times (given that the density of certain *a*MOFs has been observed to decrease with increasing milling time)[13] though no work has been performed at present.

Various routes to photoluminescent glassy materials can also be envisaged, either by amorphization of rare earth containing frameworks, by introduction of a small amount of lanthanide salt during solvothermal synthesis, or by postsynthetic ion inclusion, before thermal amorphization. Significant hurdles exist in each method, however, in avoiding phase separation and generating a sufficiently favorable binding site for the introduced cation. Tunable, optically active glasses may well be produced in a similar way, through inclusion of chiral sorbent molecules.

dx.doi.org/10.1021/ar5000314 | *Acc. Chem. Res.* 2014, 47, 1555−1562

LOOKING FORWARD: AN EMERGING FIELD

One of the major barriers to the use of *a*MOFs in practice remains the difficulty in elucidating their structural characteristics. Indeed, caution must be exercised when making the distinction between true "amorphous" frameworks and those which simply undergo a reduction in particle size upon milling. It is also true that the few detailed structural investigations of *a*ZIFs performed to date are by no means definitive, because substantial debate still exists as to the structures of amorphous materials.

These arguments not withstanding, further research directions in the field of amorphous MOFs can be anticipated. The use of amorphization as a sensor for pressure, heat, or radiation changes is plausible, given the drastic structural changes to these stimuli outlined in this Account, though developing reversibility will prove key.

Much has also been made on the rational design of MOFs and in this respect, we might look to using designed MOFs to exhibit excellent selectivity for a particular guest molecule, which we wish to then immobilize by amorphization. Currently, while good uptake for various guests may be achieved, selectivity for the guest in the presence of water is much more problematic.

The production of functional glass-like materials from crystalline MOFs is a particularly attractive and relatively facile way to make new materials, though the prospect of "designer MOF glasses" is perhaps a concept too far at this stage.

Aside from being used in practical applications themselves, the study of *a*MOFs should also prove beneficial to those researching the processing and shaping of MOF powders. Densification of MOFs is of great interest for gas storage applications, though the processing conditions that are used often result in deterioration of porous structure.[21] Similarly, applications of crystalline frameworks in high-pressure chromatography have been mooted, though knowledge of pressure-induced structural alterations is again lacking. Studies on using MOFs for optical materials (requiring transparency) will also benefit from a greater understanding of the mechanical limits of MOF structures, while sintering processes used to shape MOF powders must also avoid conditions leading to amorphization.

It is expected that the number of amorphous MOFs reported in the coming years will increase, though to what extent they might be characterized is unclear. However, it will be important that exploration of the field is performed with an end-goal in mind, because the characterization techniques involved are simply not rapid enough to support high throughput work.

Examples of the virtuous nature of extreme disorder have been presented here, though they are by no means exhaustive. It is hoped that the domain of *a*MOFs will start to attract new research and result in a multitude of novel functional amorphous materials.

AUTHOR INFORMATION

Corresponding Authors

*E-mail: tdb35@cam.ac.uk.
*E-mail: akc30@cam.ac.uk.

Author Contributions

The manuscript was written through contributions of all authors. All authors have given approval to the final version of the manuscript. All authors contributed equally.

Notes

The authors declare no competing financial interest.

Biographies

Thomas D. Bennett was born in South Shields, U.K. (1986). He read the Natural Sciences Tripos at the University of Cambridge, specializing in Chemistry, where he completed an M.Sci. project on hybrid framework materials under Paul T. Wood. After moving to the Department of Materials Science and Metallurgy, he completed a Ph.D. on the thermomechanical properties of zeolitic imidazolate frameworks, under Professor Anthony Cheetham. In 2009, he was elected to a honorary research fellowship at the Ras Al Khaimah center for advanced materials (RAK-CAM), and in 2012, he won the Panalytical prize for an outstanding contribution to X-ray diffraction. Thomas is currently a Research Fellow at Trinity Hall, University of Cambridge, and focuses on the synthesis, structure, properties, and applications of amorphous hybrid frameworks

Tony Cheetham obtained his D.Phil. at Oxford in 1971 and joined the chemistry faculty in 1974. In 1992, he took up the Directorship of the new Materials Research Laboratory at the University of California at Santa Barbara, before moving to Cambridge in 2007 to become the Goldsmiths' Professor of Materials Science. Cheetham is a Fellow of the Royal Society (1994) and several other academies and has received numerous major awards for his work in the field of inorganic and materials chemistry, including a Chemical Pioneer Award from the American Institute of Chemists (2014). He became the Treasurer and Vice-President of the Royal Society at the end of November 2012.

REFERENCES

(1) Furukawa, H.; Cordova, K. E.; O'Keeffe, M.; Yaghi, O. M. The Chemistry and Applications of Metal-Organic Frameworks. *Science* **2013**, *341*, 974−986.

(2) Bennett, T. D.; Goodwin, A. L.; Dove, M. T.; Keen, D. A.; Tucker, M. G.; Barney, E. R.; Soper, A. K.; Bithell, E. G.; Tan, J. C.; Cheetham, A. K. Structure and Properties of an Amorphous Metal-Organic Framework. *Phys. Rev. Lett.* **2010**, *104*, No. 115503.

(3) Keen, D. A.; Goodwin, A. L.; Tucker, M. G.; Hriljac, J. A.; Bennett, T. D.; Dove, M. T.; Kleppe, A. K.; Jephcoat, A. P.; Brunelli, M. Diffraction Study of Pressure-Amorphized ZrW_2O_8 Using in Situ and Recovered Samples. *Phys. Rev. B* **2011**, *83*, No. 064109.

(4) Bennett, T. D.; Simoncic, P.; Moggach, S. A.; Gozzo, F.; Macchi, P.; Keen, D. A.; Tan, J. C.; Cheetham, A. K. Reversible Pressure-Induced Amorphization of a Zeolitic Imidazolate Framework (ZIF-4). *Chem. Commun.* **2011**, *47*, 7983−7985.

(5) Bennett, T. D.; Saines, P. J.; Keen, D. A.; Tan, J. C.; Cheetham, A. K. Ball-Milling-Induced Amorphization of Zeolitic Imidazolate Frameworks (ZIFs) for the Irreversible Trapping of Iodine. *Chem.—Eur. J.* **2013**, *19*, 7049−7055.

(6) Horcajada, P.; Serre, C.; Vallet-Regi, M.; Sebban, M.; Taulelle, F.; Férey, G. Metal-Organic Frameworks As Efficient Materials for Drug Delivery. *Angew. Chem., Int. Ed.* **2006**, *45*, 5974−5978.

(7) Greaves, G. N.; Sen, S. Inorganic Glasses, Glass-Forming Liquids and Amorphizing Solids. *Adv. Phys.* **2007**, *56*, 1−166.

(8) Yaghi, O. M. Exceptional Thermal and Chemical Stability of Zeolitic Imidazolate Frameworks (ZIFs). *Proc. Natl. Acad. Sci. U.S.A.* **2006**, *103*, 10186−10191.

(9) Lohe, M. R.; Rose, M.; Kaskel, S. Metal-Organic Framework (MOF) Aerogels with High Micro- and Macroporosity. *Chem. Commun.* **2009**, 6056−6058.

(10) Goesten, M. G.; Stavitski, E.; Juan-Alcaniz, J.; Martinez-Joaristi, A.; Petukhov, A. V.; Kapteijn, F.; Gascon, J. Small-Angle X-ray Scattering Documents the Growth of Metal-Organic Frameworks. *Catal. Today* **2013**, *205*, 120−127.

(11) Bennett, T. D.; Cao, S.; Tan, J. C.; Keen, D. A.; Bithell, E. G.; Beldon, P. J.; Friscic, T.; Cheetham, A. K. Facile Mechanosynthesis of

Amorphous Zeolitic Imidazolate Frameworks. *J. Am. Chem. Soc.* **2011**, *133*, 14546−14549.
(12) Bennett, T. D.; Keen, D. A.; Tan, J. C.; Barney, E. R.; Goodwin, A. L.; Cheetham, A. K. Thermal Amorphization of Zeolitic Imidazolate Frameworks. *Angew. Chem., Int. Ed.* **2011**, *50*, 3067−3071.
(13) Cao, S.; Bennett, T. D.; Keen, D. A.; Goodwin, A. L.; Cheetham, A. K. Amorphization of the Prototypical Zeolitic Imidazolate Framework ZIF-8 by Ball-Milling. *Chem. Commun.* **2012**, *48*, 7805−7807.
(14) Chapman, K. W.; Halder, G. J.; Chupas, P. J. Pressure-Induced Amorphization and Porosity Modification in a Metal-Organic Framework. *J. Am. Chem. Soc.* **2009**, *131*, 17546−17547.
(15) Xin, Z. F.; Chen, X. S.; Wang, Q.; Chen, Q.; Zhang, Q. F. Nanopolyhedrons and Mesoporous Supra-structures of Zeolitic Imidazolate Framework with High Adsorption Performance. *Microporous Mesoporous Mater.* **2013**, *169*, 218−221.
(16) Masciocchi, N.; Ardizzoia, G. A.; LaMonica, G.; Maspero, A.; Galli, S.; Sironi, A. Metal Imidazolato Complexes: Synthesis, Characterization, and X-ray Powder Diffraction Studies of Group 10 Coordination Polymers. *Inorg. Chem.* **2001**, *40*, 6983−6989.
(17) Masciocchi, N.; Bruni, S.; Cariati, E.; Cariati, F.; Galli, S.; Sironi, A. Extended Polymorphism in Copper(II) Imidazolate Polymers: A Spectroscopic and XRPD Structural Study. *Inorg. Chem.* **2001**, *40*, 5897−5905.
(18) Nouar, F.; Eckert, J.; Eubank, J. F.; Forster, P.; Eddaoudi, M. Zeolite-like Metal-Organic Frameworks (ZMOFs) as Hydrogen Storage Platform: Lithium and Magnesium Ion-Exchange and H-2-(rho-ZMOF) Interaction Studies. *J. Am. Chem. Soc.* **2009**, *131*, 2864−2870.
(19) Hu, Y. H.; Zhang, L. Amorphization of Metal-Organic Framework MOF-5 at Unusually Low Applied Pressure. *Phys. Rev. B* **2010**, *81*, No. 174103.
(20) Zhou, Y.; Liu, C. J. Amorphization of Metal-Organic Framework MOF-5 by Electrical Discharge. *Plasma Chem. Plasma Process.* **2011**, *31*, 499−506.
(21) Zacharia, R.; Cossement, D.; Lafi, L.; Chahine, R. Volumetric Hydrogen Sorption Capacity of Monoliths Prepared by Mechanical Densification of MOF-177. *J. Mater. Chem.* **2010**, *20*, 2145−2151.
(22) Lapidus, S. H.; Halder, G. J.; Chupas, P. J.; Chapman, K. W. Exploiting High Pressures to Generate Porosity, Polymorphism, And Lattice Expansion in the Nonporous Molecular Framework Zn(CN)(2). *J. Am. Chem. Soc.* **2013**, *135*, 7621−7628.
(23) Ohara, K.; Marti-Rujas, J.; Haneda, T.; Kawano, M.; Hashizume, D.; Izumi, F.; Fujita, M. Formation of a Thermally Stable, Porous Coordination Network via a Crystalline-to-Amorphous-to-Crystalline Phase Transition. *J. Am. Chem. Soc.* **2009**, *131*, 3860−3861.
(24) Marti-Rujas, J.; Islam, N.; Hashizume, D.; Izumi, F.; Fujita, M.; Kawano, M. Dramatic Structural Rearrangements in Porous Coordination Networks. *J. Am. Chem. Soc.* **2011**, *133*, 5853−5860.
(25) Keen, D. A.; Tucker, M. G.; Dove, M. T. Reverse Monte Carlo Modelling of Crystalline Disorder. *J. Phys.: Condensed Mater.* **2005**, *17*, s15−s22.
(26) Cairns, A. B.; Goodwin, A. L. Structural Disorder in Molecular Framework Materials. *Chem. Soc. Rev.* **2013**, *42*, 4881−4893.
(27) Beake, E. O.; Dove, M. T.; Phillips, A. E.; Keen, D. A.; Tucker, M. G.; Goodwin, A. L.; Bennett, T. D.; Cheetham, A. K. Flexibility of Zeolitic Imidazolate Framework Structures Studied by Neutron Total Scattering and the Reverse Monte Carlo Method. *J. Phys.: Condensed Mater.* **2013**, *25*, No. 395403.
(28) Lau, D.; Hay, D. G.; Hill, M. R.; Muir, B. W.; Furman, S. A.; Kennedy, D. F. PLUXter: Rapid Discovery of Metal-Organic Framework Structures Using PCA and HCA of High Throughput Synchrotron Powder Diffraction Data. *Comb. Chem. High Throughput Screening* **2011**, *14*, 28−35.
(29) McMillan, P. F. Structural Studies of Silicate Glasses and Melts; Applications and Limitations of Raman Spectroscopy. *Am. Mineral.* **1984**, *69*, 622−644.
(30) Hughes, J. T.; Bennett, T. D.; Cheetham, A. K.; Nayrotsky, A. Thermochemistry of Zeolitic Imidazolate Frameworks of Varying Porosity. *J. Am. Chem. Soc.* **2013**, *135*, 598−601.
(31) Tan, J. C.; Civalleri, B.; Lin, C. C.; Valenzano, L.; Galvelis, R.; Chen, P. F.; Bennett, T. D.; Mellot-Draznieks, C.; Zicovich-Wilson, C. M.; Cheetham, A. K. Exceptionally Low Shear Modulus in a Prototypical Imidazole-Based Metal-Organic Framework. *Phys. Rev. Lett.* **2012**, *108*, No. 095502.
(32) Proietti, E.; Jaouen, F.; Lefevre, M.; Larouche, N.; Tian, J.; Herranz, J.; Dodelet, J. P. Iron-Based Cathode Catalyst with Enhanced Power Density in Polymer Electrolyte Membrane Fuel Cells. *Nat. Commun.* **2011**, *2*, No. 416.
(33) Hu, Y.; Kazemian, H.; Rohani, S.; Huang, Y. N.; Song, Y. In Situ High Pressure Study of ZIF-8 by FTIR Spectroscopy. *Chem. Commun.* **2011**, *47*, 12694−12696.
(34) Ortiz, A. U.; Boutin, A.; Fuchs, A. H.; Coudert, F. X. Investigating the Pressure-Induced Amorphization of Zeolitic Imidazolate Framework ZIF-8: Mechanical Instability Due to Shear Mode Softening. *J. Phys. Chem. Lett.* **2013**, *4*, 1861−1865.
(35) Moggach, S. A.; Bennett, T. D.; Cheetham, A. K. The Effect of Pressure on ZIF-8: Increasing Pore Size with Pressure and the Formation of a High-Pressure Phase at 1.47 GPa. *Angew. Chem., Int. Ed.* **2009**, *48*, 7087−7089.
(36) Bennett, T. D.; Tan, J. C.; Moggach, S. A.; Galvelis, R.; Mellot-Draznieks, C.; Reisner, B. A.; Thirumurugan, A.; Allan, D. R.; Cheetham, A. K. Mechanical Properties of Dense Zeolitic Imidazolate Frameworks (ZIFs): A High-Pressure X-ray Diffraction, Nanoindentation and Computational Study of the Zinc Framework Zn(Im)(2), and its Lithium-Boron Analogue, LiB(Im)(4). *Chem.—Eur. J.* **2010**, *16*, 10684−10690.
(37) Tan, J. C.; Bennett, T. D.; Cheetham, A. K. Chemical Structure, Network Topology, And Porosity Effects on the Mechanical Properties of Zeolitic Imidazolate Frameworks. *Proc. Natl. Acad. Sci. U.S.A.* **2010**, *107*, 9938−9943.
(38) Chapman, K. W.; Sava, D. F.; Halder, G. J.; Chupas, P. J.; Nenoff, T. M. Trapping Guests within a Nanoporous Metal−Organic Framework through Pressure-Induced Amorphization. *J. Am. Chem. Soc.* **2011**, *133*, 18583−18585.